HYDROLOGIC ANALYSIS OF NOACHIAN LAKES IN THE SOUTHERN HIGHLANDS OF MARS.

Y. Matsubara[1] and A. D. Howard[1], [1]Department of Environmental Sciences, University of Virginia, P.O. Box 400123, Charlottesville, VA 22904-4123, ym9z@virginia.edu.

Introduction: Despite the controversy of atmospheric conditions of early Mars, it is evident from numerous fluvial features that Mars was episodically warm enough to support an active hydrological cycle. Fluvial features that support precipitation-driven surface water flow include: large deltaic fluvial deposits[1], sediment yield sufficient to infill large crater floors [2], meandering channels with cutoffs [1, 3], tributaries starting near the divides [4, 5], valleys extending longer than hundreds of kilometers [6, 7], and a well developed valley network with locally high drainage density [2, 6-8].

Most Martian valley networks are found in older, cratered highlands of the southern hemisphere, indicating that the fluvial processes were most active during the Noachian to early Hesperian time [4, 9] when impact cratering and erosion rates were much higher. As a result, drainage basins consisted of valley networks interspersed with craters and crater basins which overflowed if contributing basin area was large enough and precipitation exceeded evaporation [5, 10]. The determination of which enclosed basin on early Mars overflowed provides information on the prevailing climate.

A hydrologic routing model was developed to estimate stream flow and lake distribution on southern highlands. Because estimates of the hydrologic parameters for early Mars are highly uncertain, we have used relative values of runoff from precipitation and evaporation expressed as the *X ratio*. Here we present our preliminary results of possible conditions required to form fluvial features seen on Mars.

The Hydrological Routing Model: Basin lakes are fed by streams, overflow from adjacent basin lakes, and/or groundwater flow. They rise and fall in response to changes in a hydrologic balance, which, for a given enclosed basin, can be expressed as:

$$V_O = V_I + (A_T - A_L)PR_B + A_L P - EA_L \qquad (1)$$

where V_O is the yearly volumetric rate of overflow from the basin, V_I is the inflow rate from adjacent basins, A_T and A_L are, respectively, the total basin and lake area, P is the average precipitation rate, R_B is the fraction of precipitation that contributes to runoff, and E is the evaporation rate [11]. Hence, any changes in precipitation, evaporation, or runoff would cause variations in lake volume and surface area and, possibly, integration or fragmentation of larger basins. This model was validated by simulating the lake distribution in the Great Basin region in western U.S. for present and the last glacial maximum conditions [12].

X Ratio. A parameter X is defined as the ratio of the net lake evaporation rate to runoff depth:

$$X = \frac{(E-P)}{PR_B} = \frac{(E/P-1)}{R_B} \qquad (2)$$

As evaporation becomes more important relative to other parameters, X gets larger and only few basins would overflow and drainage networks would be fragmentary. Conversely, all basins would overflow and most craters should have evidence of erosion by water overflowing the rim as X gets smaller. For this study, the model was run under 16 different X values, ranging from -1 to 19 with smaller increments at smaller X values. Spatially uniform values of X were assumed for each simulation, and we utilized a DEM from which large post-Noachian craters were removed and replaced with smooth topography in order to provide drainage paths more representative of Noachian conditions.

Analysis: We have examined the predicted and mapped lake distribution and how it varies as a function of the *X ratio*. Instead of looking at individual lakes, we have divided the southern highland into small cells and computed regional averages for each cell. The size of the cell used was 1332 km x 1332 km at the equator, and there was 50% overlap between adjacent cells. Two of the large basins, Hellas and Argyre, and volcanic complexes were excluded from the region of interest. Also, only the cells that covered more than 75% of Noachian cratered terrain were used for this analysis. Another criterion we have incorporated was the critical lake size. We have limited our analysis to lakes with surface area over 200 km^2 at X=4.

Lake Classifications. [10] have identified total of 221 lakes on southern highlands that showed evidence of overflow due to formation of exit breaches. We have used 146 of the 221 Fassett lakes for our analysis. Some of the Fasset lakes were excluded because they were either too small to identify at our global run resolution or they were merged as one big lake at the value of X (4.0) that we used to identify Fassett lakes. All non-Fassett lakes were classified into level-1 and level-2 lakes depending on the overflow level. Level-1 lakes are the lakes at their maximum overflow level. Some basins had overflows at higher X values as well that we call level-2 lakes.

Preliminary Results: As expected, the total number of overflowing basins larger than the critical area

increased with increasing *X ratio* at first as large lakes fragmented into smaller ones and then decreased rapidly for simulated climates too dry to form large lakes. Also, lake volume, lake area, local inflow, inflow from surrounding basin, and discharge from the lake all decreased with increasing *X ratio* (Fig. 1, results not all shown).

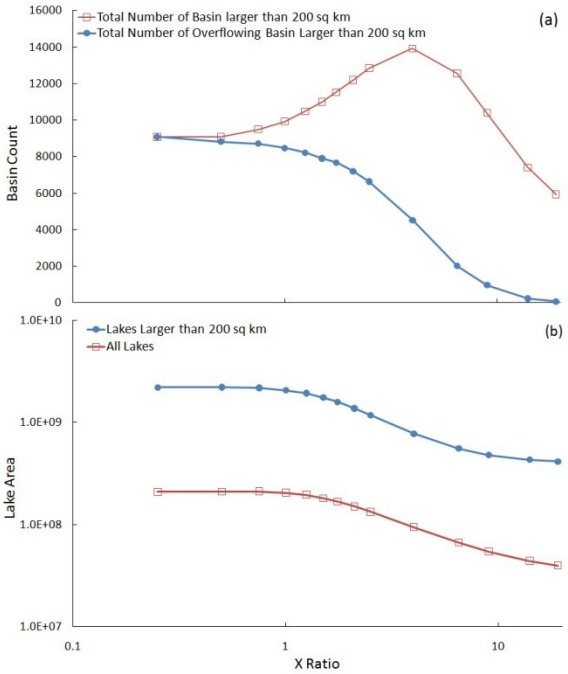

Fig. 1. Changes in (a) total number of basin (square) and overflowing basin (circle) for Lakes larger than 200 km^2 and (b) surface lake area for all lakes (square) and lakes larger than 200 km^2 (circle) with respect to X Ratio.

Figure 2 shows the regional distribution of average *X ratios* at overflow values with superimposed elevation contour lines for level-1 lakes. It is evident that regions with steep slope tend to overflow at higher *X ratios* and flatter regions require low *X ratios*. The same general trend was observed for level-2 and Fassett lakes as well (result not shown).

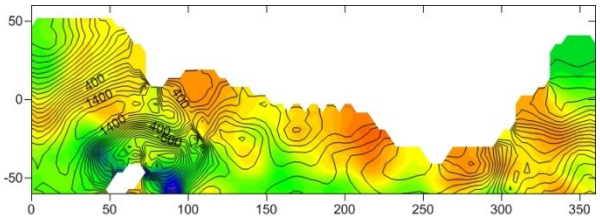

Fig. 2. Distribution map of overflow *X ratio* with elevation contour lines superimposed for level-1 lakes. *X ratio* ranges from 1.2 (purple) to 4.0 (red).

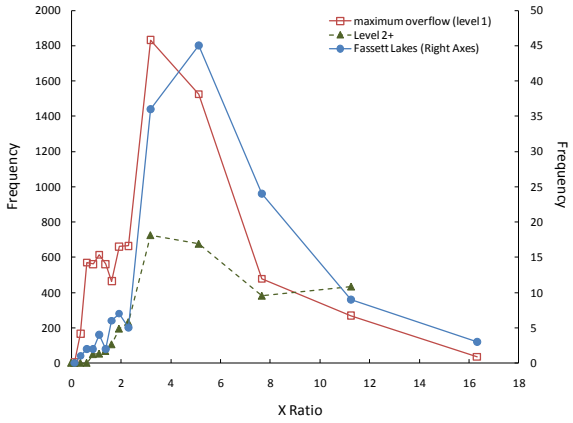

Fig. 3. X *ratio* frequency distribution for Level 1, 2+, and Fassett lakes.

The overflow *X ratio* ranged from 0.1 to 16 and most basins required the *X ratio* between 3 and 6 to have lakes of adequate size (Fig. 3). This is comparable with the *X ratios* for the Great Basin during the last glacial maximum. The *X ratios* computed for Pleistocene Lakes Bonneville (western Utah), Lahontan (western Nevada), and Manly (Death Valley, CA) are 1.8, 4.5, and 6.8, respectively.

Our results also show that frequency distribution of overflow *X ratios* for Fassett and level-1 lakes are very similar (Fig. 3). The mean *X ratio* for Level-1 and Fassett lakes are 3.19 and 4.96, respectively. This implies that climatic conditions required to cause overflow of the Fassett lakes would have caused high lake levels in most basins and suggests that additional basins in the southern highlands overflowed but not intensely enough or frequently enough to form obvious exit breaches. As a continuation of this work, we will be comparing predicted path and intensities of simulated surface flows with the distribution and depth of incision of highland valley networks.

References: [1] Moore J.M. et al. (2003) *GRL*, *30(24)*, 2292, doi:10.1029/2003GL019002. [2]Howard A.D. et al. (2005) *JGR*, *110*, D12S14, doi:10.1029/2005JE002459. [3] Malin M.C. and Edgett K.S. (2003) *Science*, *302*, 1931-1934. [4] Irwin R.P. III et al. (2005) *Geology*, *33*, 489-492. [5] Irwin R.P. III et al. (2005) *JGR*, *110*, E12S15, doi:10.1029/2005JE002460. [6] Mangold N. et al. (2004) *Science*, *305*, 78-81. [7] Hynek B.M. and Phillips R.J. (2003) *Geology*, *31(9)*, 757-760. [8] Quantin C. et al. (2005) *JGR*, *110*, E12S19, doi:10.1029/2005JE002440. [9] Grant J.A. (2000) *Geology*, *28(3)*, 223-226. [10] Fassett C.I. and Head J.W. (2008) *Icarus*, *198,* 37-56. [11] Howard A.D. and Matsubara Y. (2006) *LPSC XXXVII*, Abstract # 1209. [12] Matsubara Y. and Howard A.D. (2009) *Water Resour. Res., 45,* W06425, doi:10.1029/2007WR005953.